

# A strategy for the spatial temperature control of a molten carbonate fuel cell system

Min Sheng<sup>a,\*</sup>, Michael Mangold<sup>a</sup>, Achim Kienle<sup>a,b</sup>

<sup>a</sup> Max-Planck-Institute for Dynamics of Complex Technical Systems, Sandtorstraße 1, 39106 Magdeburg, Germany

<sup>b</sup> Otto-von-Guericke-University Magdeburg, Chair for Automation/Modelling, Universitätsplatz 2, 39106 Magdeburg, Germany

Received 28 February 2006; received in revised form 25 July 2006; accepted 23 August 2006

Available online 28 September 2006

## Abstract

The object of the paper is to develop a simple and practical control strategy for a molten carbonate fuel cell (MCFC) system. Based on a dynamic model and the control demand, a cascade control strategy is designed. The master controller imposes a change of cell current representing a change in power demand and sets the amount of fuel gas, the steam-to-carbon ratio, the air number and the cathode gas recycle ratio to their corresponding conditions for optimal steady state electric efficiency. Two feedback PID controllers are in the inner loop, one guarantees the solid temperature not to exceed a maximum temperature by changing the air number around the default set by the master controller; the other controls the maximum temperature difference by adjusting the steam-to-carbon ratio. Step response tests show that this control strategy works well when the cell current changes.

© 2006 Elsevier B.V. All rights reserved.

**Keywords:** Molten carbonate fuel cell; Dynamic model; Cascade control; PID controller; Temperature control

## 1. Introduction

Molten carbonate fuel cells (MCFC) are a moderate to high temperature fuel cell technology. The nominal operating temperature is around 600 °C, which is the typical operating temperature found in conventional utility power plants. Theoretically, the MCFC has a high fuel-to-electricity efficiency (~55–60%) and minimal environmental emissions such as nitrogen oxides (NO<sub>x</sub>) (<1 ppm). These properties make the MCFC an attractive candidate for decentralized power generation [1].

An industrial MCFC stack is characterized by a high degree of system integration, as the process behavior depends on numerous interactions between the electrochemical reaction steps, the internal reforming, mass transport processes, and the heat transfer inside a cell or stack. An understanding of the physical–chemical processes in an MCFC can be obtained from mathematical models based on physical conservation principles [2]. Model-based process control and process design strategies

can lead to a much better use of the fuel cells' capacities and increase the efficiency of the system.

As the overall fuel-to-electricity conversion efficiency is the most concerned interest for power industries, a maximum electric efficiency is desired not only when the cell is operated at constant load over a long period of time but also during dynamic load changes. In the former situation, an optimal electric efficiency can be achieved through a steady state optimization procedure [2]; whilst in the latter situation a fast and safe transition must also be taken into consideration. To keep the process safe, the solid temperature must not exceed a minimum and a maximum temperature, and also the maximum temperature difference within the solid phase is limited. In literature, only a few publications about model-based control of MCFC are available. Lucas and Lee [3] describe a first principle-based non-linear dynamic model and also obtain reduced-order models, but no spatial gradients are considered. Kang et al. [4] derive a linear 3 × 3 transfer function matrix model from experimental study, which will simplify the design of controllers but will limit the control to the vicinity of a chosen operating point. Shen et al. [5] present an adaptive fuzzy control procedure for the temperature of MCFC stack based on a neural network identification model. As the dynamic model is also empirical, the applicability of the con-

\* Corresponding author. Tel.: +49 391 6110388; fax: +49 391 6110577.  
E-mail address: [sheng@mpi-magdeburg.mpg.de](mailto:sheng@mpi-magdeburg.mpg.de) (M. Sheng).

### Nomenclature

$I_{\text{cell}}$	total cell current
S/C	steam-to-carbon ratio
$\tilde{S}/\tilde{C}$	steam-to-carbon ratio estimated from steady state optimization
$U_{\text{cell}}$	cell voltage

### Greek symbols

$\Gamma_{\text{feed}}$	amount of fuel gas
$\eta_{\text{el}}$	electric efficiency optimized
$\tilde{\eta}_{\text{el}}$	electric efficiency controlled
$\vartheta_{\text{diff}}$	maximum temperature difference
$\vartheta_{\text{max}}$	maximum temperature
$\vartheta_{\text{min}}$	minimum temperature
$\lambda_{\text{air}}$	air number and cathode gas recycle ratio
$\tilde{\lambda}_{\text{air}}$	air number and cathode gas recycle ratio estimated from steady state optimization

troller is restricted to operation conditions, where this model is valid. This work tries to construct a framework for satisfying high electric efficiency over a larger range of operation points and at the same time controlling the solid temperature when power load changes. For simulation, optimization and control of MCFC processes mathematical models are required. Firstly, the paper summarizes a detailed spatially two-dimensional model of the MCFC presented in previous publications [2,6]. A control strategy is then constructed which achieves the optimal electric efficiency by a steady state optimization and at the same time satisfies the solid temperature constraints by involving two PID controllers.

Currently, the combination of independently designed feed-forward and feedback controllers [12] is attracting increasing attention as a control concept for nonlinear systems [13]. Aguiar et al. [14] use such a concept for the control of the outlet fuel temperature of a SOFC and test the controller in simulations with a spatially one-dimensional model. Spatial temperature gradients are monitored in [14], but it is not tried to control them directly.

As will be shown in the later sections, the control approach proposed in this paper includes the control of spatial dependencies (the control of stack temperature difference). It combines a feed-forward branch based on a detailed physical model and feedback PID controllers. In practice, a suitable state estimator as presented in [6,10] will make the control method applicable, if the maximum temperature and the maximum spatial temperature difference cannot be measured.

The application example considered in this paper is the so-called HotModule by MTU CFC Solutions [7]. The HotModule is an integrated MCFC system with a cell stack of 342 fuel cells that can deliver up to 250 kW of electrical power. A pilot plant installation of the HotModule exists at the Magdeburg university hospital, Germany. This pilot plant has been subject of a joint research project of several academic and industrial partners that aimed at model development and model-based process control [6]. Within this project, the HotModule has been used for experi-

mental validation of the developed physical models [2] and state estimators [6,10]. The controller presented here is an extension of the results obtained in the project.

## 2. Dynamic model

### 2.1. Working principle of an MCFC

Fig. 1(a) shows the principle of an MCFC with direct internal reforming (DIR). The MCFC consists of two porous electrodes, an electrolyte layer between them and gas channels above each electrode. The anode channel is fed with a mixture of natural gas (methane) and steam. In an internal reforming step, the reactions are oxidized to hydrogen and carbon monoxide. Both are oxidized electrochemically at the anode, consuming carbonate ions from the electrolyte and producing free electrons.

On the cathode side, new carbonate ions are formed in a reduction reaction under consumption of electrons from the electrode. The electrons from the anode are transferred to the cathode via an external electric circuit, where they perform electric work.

In this work, a MCFC system is considered, whose simplified scheme is depicted in Fig. 1(b). The fresh anode feed consisting of steam and methane first enters a pre-reformer where a part of the methane is converted to hydrogen, and then is distributed to the anode gas channels of the cell stack. The outlet flow on anode side goes into a burner. The burner is supplied with air from the ambient and oxidizes unconsumed methane and hydrogen. The burner outlet is fed to the cathode gas channels. Finally, a part of the cathodic exhaust gases may be recycled to the burner.

### 2.2. Two-dimensional spatially distributed MCFC model

A detailed model of a planar fuel cell with cross flow has been derived from first principles [8,9]. The model is dynamic and spatially distributed in two space coordinates. The main model assumptions are:

- Isobaric gas phases, ideal gas law.
- Plug flow in all channels.
- All immobile parts of the cell, i.e. electrodes, electrolyte, bipolar plates, etc. are lumped into a solid phase with respect to their enthalpy balance.
- Reversible potential kinetics for reforming reactions, Butler–Volmer kinetics for electrochemical reactions. All kinetics feature an Arrhenius term.
- The electric potential field is spatially distributed and allows for the calculation of an inhomogeneous current density distribution.
- Mass transport resistance in the electrode pores is considered.

The resulting model is a system of hyperbolic and parabolic partial differential equations for the temperatures in the gas and solid phases, for the composition of the gases, and for the electrical potentials. A reduced version of the model, which is more suitable for process control purposes, has been derived in [10,11].

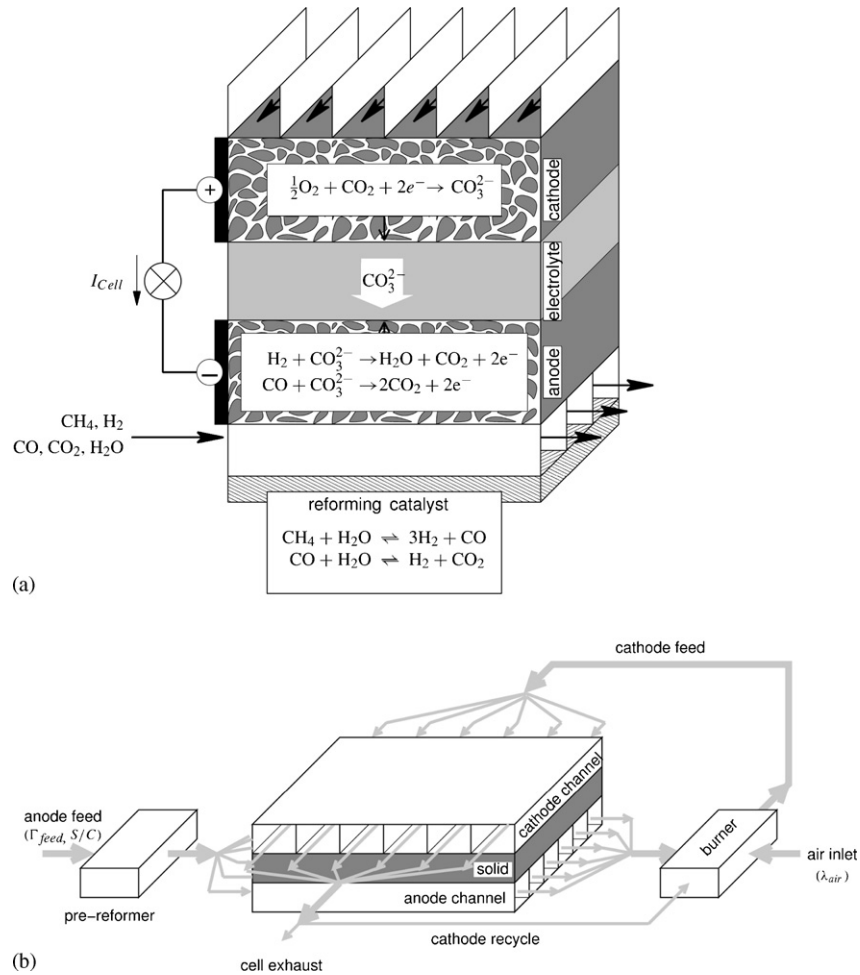


Fig. 1. (a) Working principle of an MCFC with direct internal reforming (DIR) and (b) scheme of the MCFC system considered in this work, which consists of a pre-reformer, the cell stack, and a burner between anode side and cathode side.

### 3. The control strategy

The model described in Section 2 gives the basis to design a control strategy. A fast and safe dynamic response during the cell current change is necessary. As the power load does not change very frequently an optimal steady state electric efficiency is also desired. In the ideal case the electric efficiency is dynamically optimized such that both demands can be achieved at the same time. However, the optimization of a complex non-linear fuel cell model in real time is very difficult. To overcome this problem, the approach adopted here is to achieve the optimal state electric efficiency in offline optimization and then to make sure that the dynamic response is as fast and safe as possible. That is, when the power load changes (i.e. the cell current changes) a master loop switches the operating variables to their new static conditions that satisfy an optimal electric efficiency at the new load. Then in the inner loop feedback controllers satisfy the dynamic performance criteria. In the following, steady state optimization will be introduced first and temperature response tests will then be performed in order to decide which operating variable controls which controlled variable. Control schematic and results will be given thereafter.

This approach is similar to the control concept proposed by Aguiar et al. for an SOFC stack [14]. However, in contrast to [14], a spatially two-dimensional temperature field is considered in this work. Furthermore, the concept proposed here controls the maximum temperature and the maximum spatial temperature difference at the same time. This leads to a multiple-input/multiple-output (MIMO) control problem, where the choice of suitable manipulated variables is more difficult than in the single-input/single-output case.

#### 3.1. Steady state optimization

Heidebrecht [2] optimizes the input parameters of a single cross flow cell at given cell current to yield an optimal electric efficiency while fulfilling several temperature restrictions and avoiding carbonization in the anode channel. The optimization is performed at different cell currents, so that several points of a current–voltage curve with optimal operating conditions are evaluated.

The electric efficiency, which is used as the objective function of the optimization relates the total electric cell power diminished by the system's parasitic power consumption to the

combustion enthalpy input of the fuel gas. The optimization has several constraints concerning the solid temperature and the possibility of carbonization. The temperature must not exceed a minimum and a maximum temperature, and also the maximum temperature difference within the solid phase is limited. Three operation parameters, which can be adjusted easily in the HotModule, are chosen as optimization variables (cf. Fig. 1b). The first optimization variable is the total amount of fuel gas ( $\Gamma_{\text{feed}}$ ) fed to the system. In the case of the HotModule, the fuel gas consists of steam and methane. The ratio between the flux of steam and the flux of methane fed to the system, i.e. the steam-to-carbon ratio (S/C), is chosen as the second optimization variable. It should be noted that water is generated in the anodic reaction and consumed in the internal reforming step. Therefore, the amount of water in the system affects the reforming reaction as well as the electrochemical reaction. The interaction between the exothermic anodic reaction and the endothermic reforming step strongly influences the temperature in the cell. Therefore, the steam-to-carbon ratio has a strong impact on the overall system behavior and can be seen as one of the most important operation parameters. This is also reflected by the fact that in the case of the HotModule the steam-to-carbon ratio can be set directly at the process control system. The third optimization variable is the air number ( $\lambda_{\text{air}}$ ), defined as the ratio between the amount of air actually fed to the burner and the amount of air required under stoichiometric conditions. Those three variables must be adjusted to meet the power demands from an external load on the cell in an optimal way. For simplicity, the effect of the external load is modeled by setting the total cell current ( $I_{\text{cell}}$ ) to a fixed value within each optimization.

Some typical input quantities at the optimum points together with additional information like temperature are listed in Table 1. For the control purpose the number of steady state optimization points should be infinite to obtain optimal steady state performance at arbitrary cell currents. In order to have more possible operation points the table by Heidebrecht [2] was extended by specifying  $I_{\text{cell}}$  change by 0.01 from 0.5 to 1.0. When an  $I_{\text{cell}}$  change is less than 0.01, the optimized variable values between two nearest points are interpolated. For an  $I_{\text{cell}}$  change, the master controller looks up the table, locates the column of the desired  $I_{\text{cell}}$  state and sets the three variables ( $\Gamma_{\text{feed}}$ , S/C,  $\lambda_{\text{air}}$ ) to their corresponding numbers.

Table 1  
Results of the steady state optimization of input parameters

$I_{\text{cell}}$	0.5	0.6	0.7	0.8	0.9	1.0
$\Gamma_{\text{feed}}$	0.6783	0.8296	0.9841	1.114	1.2859	1.2920
S/C	2.4304	2.4707	2.4903	2.4321	2.3106	1.7049
$\lambda_{\text{air}}$	2.0250	2.0659	2.1913	2.3447	2.6071	2.9574
$\vartheta_{\text{min}}$	2.9604	2.9999	2.9999	2.9919	2.9942	3.0000
$\vartheta_{\text{max}}$	3.1604	3.2000	3.1999	3.1994	3.2017	3.2000
$\vartheta_{\text{diff}}$	0.2000	0.2001	0.2001	0.2075	0.2076	0.2000
$\eta_{\text{el}}$	0.5391	0.5240	0.5030	0.4809	0.4384	0.3838
$\tilde{\eta}_{\text{el}}$	0.5391	0.5240	0.5030	0.4769	0.4352	0.3838

$\tilde{\eta}_{\text{el}}$  refers to the closed-loop case discussed in Section 3.4.

### 3.2. Solid temperature response analysis

The control object is to fulfill the temperature constraints when the current load changes, that is, to transfer the fuel cell safely from an optimal steady state to another. The steady state optimization introduced in the previous section gives a reference of what the input parameters ( $\Gamma_{\text{feed}}$ , S/C and  $\lambda_{\text{air}}$ ) would be like to achieve the desired new state, but the dynamics of transition do not guarantee the temperature constraints. In order to control the solid phase temperature during dynamic transition, temperature control loops are required. The possible controlled variables are minimum temperature ( $\vartheta_{\text{min}}$ ), maximum temperature ( $\vartheta_{\text{max}}$ ) and maximum temperature difference ( $\vartheta_{\text{diff}}$ ). It is found that the minimum temperature rarely exceeds the limits, so there are two controlled variables ( $\vartheta_{\text{max}}$  and  $\vartheta_{\text{diff}}$ ) and as stated already three manipulated variables ( $\Gamma_{\text{feed}}$ , S/C and  $\lambda_{\text{air}}$ ). This is a typical multi-input–multi-output (MIMO) control problem. In the following, a match of input and output variables based on physical considerations is attempted. Dynamic responses of the system model to step changes of the three manipulated variables are considered. Fig. 2 shows the step responses of all the possible input and output matches when each of the three input variables changes from its corresponding optimized state at  $I_{\text{cell}} = 0.8$  to the optimized state at  $I_{\text{cell}} = 0.7$  at time 5000 and then changes back to the optimized state at  $I_{\text{cell}} = 0.8$  at time 10,000. The actual cell current is kept constant at  $I_{\text{cell}} = 0.8$ . All results are given in dimensionless numbers, one dimensionless time unit corresponding to 66 s. For the cell current and the temperature, the following scaling is used: one current density unit equal to 840 A m<sup>-2</sup>, one temperature unit equal to 273 K.

Fig. 2(a) gives the temperature difference and maximum temperature response when switching  $\Gamma_{\text{feed}}$  from its optimal state (1.114) to the new optimal state (0.9841) while keeping  $\lambda_{\text{air}}$  and S/C at their old state. A reduction of  $\Gamma_{\text{feed}}$  means physically that less fuel is fed to the system. As the cell current is kept constant and the cell voltage changes only slightly, the electrical power hardly varies during the simulation experiment in Fig. 2(a). Consequently, the reduction of  $\Gamma_{\text{feed}}$  results in a higher electrical efficiency and – because less chemical energy is converted to heat – in a lower average temperature of the stack. However, the new steady state with the higher efficiency, which is reached at time ~6000, is not feasible as the temperature difference is above the tolerable limit. This behavior is found to be typical for changes of  $\Gamma_{\text{feed}}$  at different operation points. A reduction of  $\Gamma_{\text{feed}}$  by a small amount always leads to a spatially more inhomogeneous temperature profile and hence to an increase of the maximum spatial temperature difference. The implications of a modified  $\Gamma_{\text{feed}}$  on the absolute maximum temperature are less clear. Depending on the actual operation point, the temperature maximum may increase or decrease. Therefore,  $\Gamma_{\text{feed}}$  is a suitable variable for controlling the temperature difference but is not suitable for controlling the maximum temperature.

The system response to a variation of the steam-to-carbon ratio is qualitatively similar to the response to a variation of  $\Gamma_{\text{feed}}$ . An Example is shown in Fig. 2(b). An increase of S/C at a constant  $\Gamma_{\text{feed}}$  also means a reduction of the amount of fuel fed to the system. Therefore, the argumentation used to

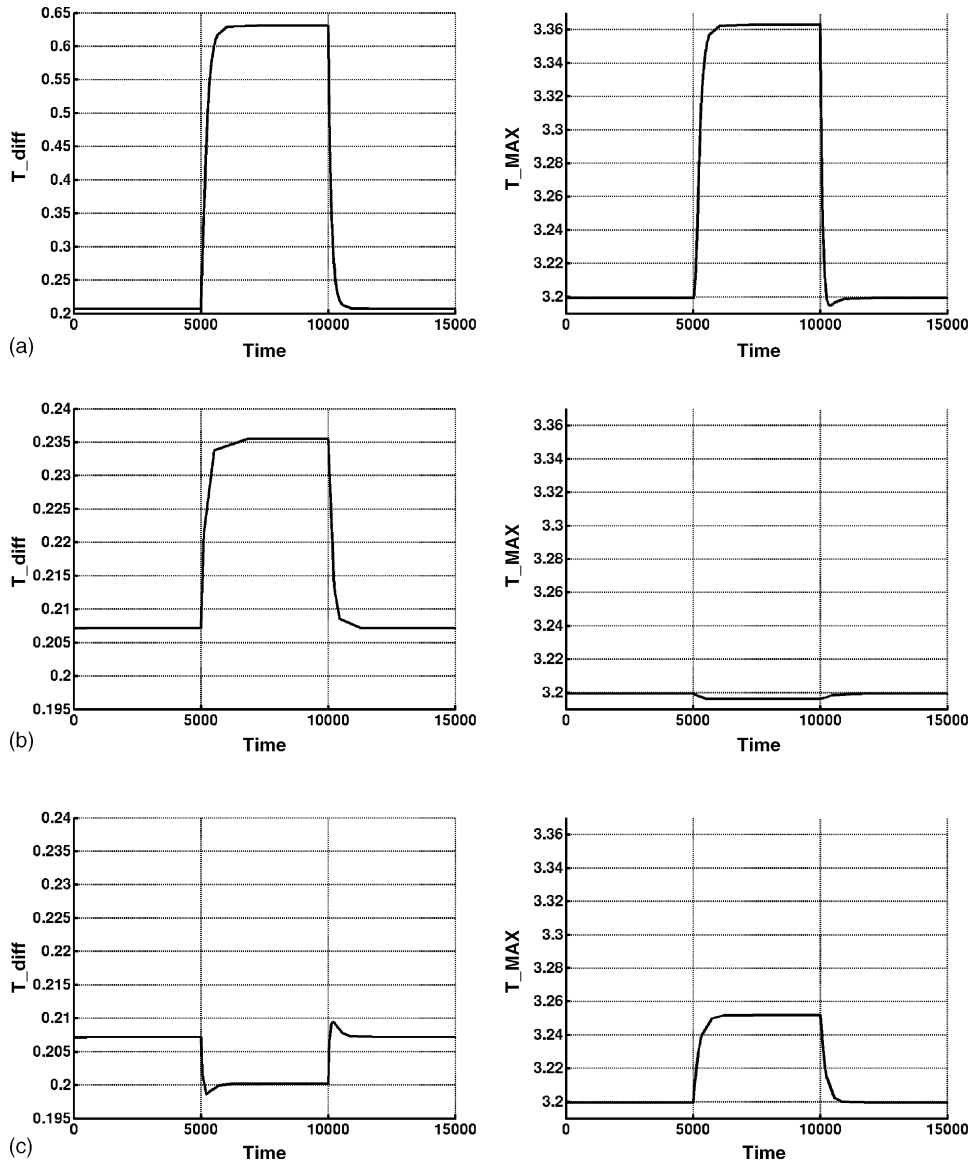


Fig. 2. (a)  $\vartheta_{max}$ ,  $\vartheta_{diff}$  response to a  $\Gamma_{feed}$  change;  $\Gamma_{feed}$  changes at from the optimal value at  $I_{cell} = 0.8$  to the optimal value at  $I_{cell} = 0.7$  and back again. (b)  $\vartheta_{max}$ ,  $\vartheta_{diff}$  response to a S/C change; S/C changes at from the optimal value at  $I_{cell} = 0.8$  to the optimal value at  $I_{cell} = 0.7$  and back again. (c)  $\vartheta_{max}$ ,  $\vartheta_{diff}$  response to a  $\lambda_{air}$  change;  $\lambda_{air}$  changes at from the optimal value at  $I_{cell} = 0.8$  to the optimal value at  $I_{cell} = 0.7$  and back again.

explain Fig. 2(a) holds for (b), too. An increase of S/C generally causes an increase of the temperature difference, while the maximum temperature may decrease or increase, depending on the operation point. Therefore, the steam-to-carbon-ratio is another possible candidate for the control of the spatial temperature difference.

The effect of a varying air number  $\lambda_{air}$  is shown in Fig. 2(c). A higher amount of air in the system mainly has a cooling effect, i.e. it reduces the maximum temperature. The influence on the spatial temperature difference is not that strong. Therefore, varying  $\lambda_{air}$  locally around a given set-point is a good method to control the maximum temperature of the fuel cell.

To summarize the discussion of Fig. 2, the air number  $\lambda_{air}$  has the most direct relationship to  $\vartheta_{max}$  because of its cooling effect. As to  $\vartheta_{diff}$ , the effect of  $\Gamma_{feed}$  and S/C is almost the same and in this work S/C is chosen to control  $\vartheta_{diff}$ . The resulting cascade

control scheme is depicted in Fig. 3. A feed-forward controller sets the three manipulated variables  $\Gamma_{feed}$ ,  $\lambda_{air}$ , S/C to the optimal steady state values  $\tilde{\Gamma}_{feed}$ ,  $\tilde{\lambda}_{air}$ ,  $\tilde{S/C}$ . The air number  $\lambda_{air}$  is tuned by the PID controller 1 around the default set by the feed-forward controller in order to obtain a pre-defined maximum solid temperature  $\vartheta_{max}$  also under transient conditions; similarly, S/C is tuned by PID controller 2 around the optimum steady state value in order to achieve a pre-defined maximum temperature difference  $\vartheta_{diff}$ .

### 3.3. Control results and analysis

Fig. 4(a) and (b) present the  $\vartheta_{diff}$  and  $\vartheta_{max}$  transient behavior, under open-loop and closed-loop conditions, when the cell current changes from 0.55 to 0.6 and further to 0.65, 0.75, 0.8, 0.85, 0.9, 0.95, 1.0 at every 2000 time units (0, 2000, . . . , 18,000) rep-

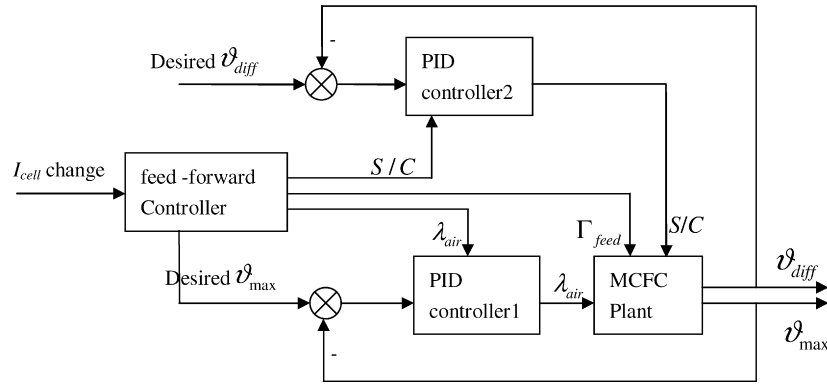


Fig. 3. The cascade control scheme.

representing positive load changes and then changes back from 1.0 to 0.95, 0.9, . . . , 0.5 at times (20,000, 22,000, . . . , 38,000) representing negative load changes. Note that closed-loop implies that all control loops are active, whereas open-loop suggests that only the master controller is in operation.

The following parameters of the PID controllers are used:  $\vartheta_{diff}$  controller gain = 180.0, integral time = 20.0, derivative time = 500.0;  $\vartheta_{max}$  controller gain = 24.0, integral time = 0.29, derivative time = 40.0. These parameter values are found to provide a satisfactory system response. As can be seen, for the open-loop case (no temperature control),  $\vartheta_{diff}$  and  $\vartheta_{max}$  usually exceed their corresponding limits (0.2 and 3.2, respectively), while for closed-loop case, the PID controllers successfully and quickly bring the temperatures back to their desired set-points.

In the simulation shown in Fig. 4, the desired  $\vartheta_{diff}$  was always set to 0.2, resulting in a steady state electric efficiency deviating slightly from the optimal value, as can be seen from Table 1.

### 3.4. State estimator

Usually, the required measurement information on  $\vartheta_{diff}$  and  $\vartheta_{max}$  is not directly available from an industrial fuel cell system. In most cases, temperature measurements can be taken only at a few points in the cell stack. To make the proposed control scheme applicable in practice, a state estimator or observer is required. Such state estimation techniques were developed in previous work [6,10] based on a reduced MCFC model [11]. It could be shown that the developed observers provide accurate

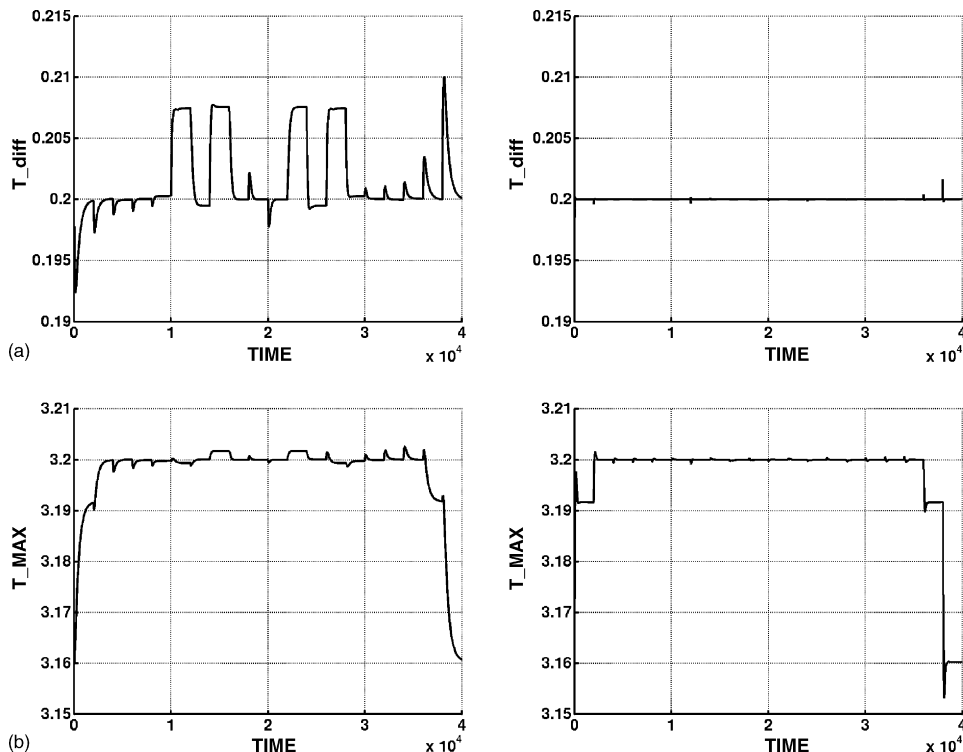


Fig. 4. (a)  $\vartheta_{diff}$  control results (open-loop on left panel and closed-loop on right panel) and (b)  $\vartheta_{max}$  control results (open-loop on left panel and closed-loop on right panel).

estimates of the spatial temperature profile, but use only a small amount of CPU time.

#### 4. Conclusions and outlook

In open literature, comparatively few publications are available on model-based process control of MCFC systems. The results of this work show that a rather simple control scheme can contribute substantially to a safe and efficient operation of a high temperature fuel cell stack. Such systems are rather sensitive to local over-temperatures and spatial temperature differences. Therefore, temperature management is a key problem of the process operation of high temperature fuel cells. This work proposes a cascade control scheme that may overcome this problem. The cascade control consists of three control loops. The first loop is composed of a master (feed-forward) controller that imposes a load change and sets the fuel gas, the steam-to-carbon ratio, and the air number to their corresponding conditions for optimal steady state electric efficiency. The master-controller reads the steady state operation conditions from a look-up table. In this work, the look-up table was generated by optimizing the steady state solutions of a detailed process model; alternatively, it would also be possible to determine optimal steady state operation conditions experimentally and store them in the look-up table.

The other two loops are feedback PID controllers that are responsible for the temperature management under transient conditions. One of the PID controllers adjusts the air number in order to keep the maximum temperature below a pre-defined limit. The other PID controller corrects the steam-to-carbon ratio in order to limit the maximum spatial temperature difference. This simple control structure with linear feed-back controllers is inspired by the physical properties of the system and offers several advantages. Firstly, the actions of the controller appear to be transparent and understandable to the operating personal, a demand often made by practitioners on advanced control schemes. Secondly, the scheme has been derived from rather general properties of high temperature fuel cells and, therefore, may be robust to model uncertainties and applicable to many fuel cell systems.

The implementation of the developed cascade control is especially simple, if it is possible to measure directly the maximum temperature and the maximum temperature difference, as was assumed in this work. In practice, this measurement information is not always available. Very often, temperature measurements

can only be taken at the outlets of the gas channels or at a few distinct points within the cell stack. In such cases, it is possible to estimate the desired maximum temperatures and temperature differences with good accuracy from the available measurement information by using state estimation techniques. This was demonstrated in previous publications [6,10]. In a next step, the controller developed here will be combined with a suitable state estimator in order to make the scheme applicable under conditions, where measurement information is limited.

#### References

- [1] San Diego Gas & Electric, Report on molten carbonate fuel cell development and demonstration, 1999.
- [2] P. Heidebrecht, Modelling, Analysis and Optimisation of a Molten Carbonate Fuel Cell with Direct Internal Reforming (DIR-MCFC), Fortschritt-Berichte/VDI-Verlag, Düsseldorf, 2005.
- [3] M.D. Lukas, K.Y. Lee, Model-based analysis for the control of molten carbonate fuel cell systems, *Fuel Cells* 5 (2005) 115–125.
- [4] B.S. Kang, J.-H. Koh, H.C. Lim, Experimental study on the dynamic characteristics of kW-scale molten carbonate fuel cell systems, *J. Power Sources* 94 (2001) 51–62.
- [5] C. Shen, G.-Y. Cao, X.-J. Zhu, X.-J. Sun, Nonlinear modeling and adaptive fuzzy control of MCFC stack, *J. Process Contr.* 12 (2002) 831–839.
- [6] M. Mangold, M. Sheng, P. Heidebrecht, A. Kienle, K. Sundmacher, Development of physical models for the process control of a molten carbonate fuel cell system, *Chem. Eng. Sci.* 59 (2004) 4847–4852.
- [7] M. Bischoff, G. Huppmann, Operation experience with a 250 kW<sub>el</sub> molten carbonate fuel cell (MCFC) power plant, *J. Power Sources* 105 (2002) 216–221.
- [8] P. Heidebrecht, K. Sundmacher, Dynamic modelling and simulation of a counter current molten carbonate fuel cell (MCFC) with internal reforming, *Fuel Cells* 2 (2003) 166–180.
- [9] P. Heidebrecht, K. Sundmacher, Molten carbonate fuel cell (MCFC) with internal reforming: model-based analysis of cell dynamics, *Chem. Eng. Sci.* 58 (2003) 1029–1036.
- [10] M. Grötsch, M. Gundermann, M. Mangold, A. Kienle, K. Sundmacher, Development and experimental investigation of an extended Kalman filter for a molten carbonate fuel cell system, *J. Process Contr.* 16 (2006) 985–992.
- [11] M. Mangold, M. Sheng, Nonlinear model reduction of a two-dimensional MCFC model with internal reforming, *Fuel Cells* 4 (2004) 68–77.
- [12] I.M. Horowitz, *Synthesis of feedback systems*, Academic Press, New York, 1963.
- [13] K. Graichen, V. Hagenmeyer, M. Zeitz, A new approach to inversion-based feedforward control design for nonlinear systems, *Automatica* 41 (2005) 2033–2041.
- [14] P. Aguiar, C.S. Adjiman, N.P. Brandon, Anode-supported intermediate temperature direct internal reforming solid oxide fuel cell II. Model-based dynamic performance and control, *J. Power Sources* 147 (2005) 136–147.